REPRODUCTION
RESEARCH

The polymorphism of rs6505162 in the *MIR423* coding region and recurrent pregnancy loss

Xing Su[1,2,*], Yi Hu[1,2,*], Ying Li[1,2], Jing-Li Cao[1,2], Xue-Qin Wang[1,2], Xu Ma[1,2] and Hong-Fei Xia[1,2]

[1]*Reproductive and Genetic Center of National Research Institute for Family Planning, Beijing 100081, China and* [2]*Graduate School, Peking Union Medical College, Beijing, China*

Correspondence should be addressed to X Ma; Email: genetic@126.com or to H-F Xia; Email: hongfeixia@126.com

*(X Su and Y Hu contributed equally to this work)

Abstract

Although the relationship between polymorphisms in microRNAs (miRNAs) and recurrent pregnancy loss (RPL) has been studied, there is very little data available in the literature. In the present study, we scanned 55 potentially functional polymorphisms in the miRNA coding region in Chinese women with unexplained RPL (URPL; no. 2011-10). The rs6505162 C>A in the *MIR423* coding region was found to be significantly associated with the occurrence of human URPL. The rare A allele contributed to an increase in the expression of mature *MIR423*. C to A substitution in the polymorphism rs6505162 in pre-*MIR423* repressed cell proliferation and migratory capacity. Further investigations showed that *MIR423* could inversely regulate the expression of proliferation-associated 2 group 4 (*PA2G4*) by binding the 3′-UTR of *PA2G4*. Dual-luciferase assay indicated that the A allele in the polymorphism rs6505162 could more effectively suppress the expression of *PA2G4* than the C allele could. Collectively, the present data suggest that rs6505162 C>A in pre-*MIR423* may contribute to the genetic predisposition to RPL by disrupting the production of mature *MIR423* and its target gene, which consequently interferes with *MIR423* functioning.
Reproduction (2015) **150** 65–76

Introduction

Early pregnancy loss is the most common complication in human reproduction, with an incidence that ranges from 50 to 70% of all conceptions (Rai & Regan 2006). Up to 5% of women experience early spontaneous pregnancy loss at least twice. Recurrent pregnancy loss (RPL) has been defined as two or more consecutive pregnancy losses (Practice Committee of American Society for Reproductive Medicine 2013). The known risk factors for RPL include advanced maternal age, maternal anatomic anomalies, chromosomal abnormalities, endocrine dysfunction, immunologic problems, environmental factors, and anti-phospholipid antibody syndrome (Rai & Regan 2006). In ∼50% of cases, the cause is not identified; this is defined as unexplained RPL (URPL), and it may result in an increased risk of women developing clinical depression and anxiety (Regan & Rai 2000, Craig *et al*. 2002).

MicroRNAs (miRNAs) are small but powerful non-coding RNA molecules that function as negative regulators of the expression of their target genes (Hinske *et al*. 2010). Most metazoan miRNAs bind to the 3′-UTRs of target mRNAs; however, there are also cases in which miRNAs regulate mRNA targets through binding sites in 5′-UTRs or coding regions (Kloosterman *et al*. 2004, Lytle *et al*. 2007). Increasing evidence has shown that single nucleotide polymorphisms (SNPs) or mutations in miRNA coding regions may alter miRNA expression and/or maturation, which may affect the occurrence of diseases (Saunders *et al*. 2007, Jazdzewski *et al*. 2008). Our previous report (Hu *et al*. 2011) showed that two SNP sites in the pre-*MIR125A* coding region are related to human RPL, which means that miRNAs might play an important role in the occurrence of RPL.

In the present study, in order to obtain a better understanding of the relationship between miRNA polymorphisms and PRL, 55 potentially functional polymorphisms were investigated in a case–control study in RPL patients from northern China. Adjusted odds ratios (ORs) were used to calculate the association between miRNA polymorphisms and PRL. The functional significance of the polymorphism of rs6505162 in the *MIR423* coding region was studied. To our knowledge, the present study is the first to systematically evaluate the impact of genetic polymorphisms in miRNA coding genes on the risk of RPL.

ISSN 1470–1626 (paper) 1741–7899 (online)
DOI: 10.1530/REP-15-0007
Online version via www.reproduction-online.org

Materials and methods

Subjects

One hundred and seventy-five RPL patients with two or more consecutive spontaneous abortions and 201 healthy controls were recruited from Ningxia Medical University. Two or more consecutive missed abortions was considered as RPL. The decidual tissues of 11 patients with two or more consecutive missed abortions and 11 healthy pregnant time-matched controls were collected from the Sixth Hospital of Shijiazhuang. The decidual tissues from the control group were mainly derived from therapeutic abortions that were executed when there was a severe threat to the mother's health or life, such as an accident or a serious pregnancy response. We excluded many factors that were likely to cause this medical condition by blood tests of the maternal blood, including a virus infection (TORCH) test, an immune antibodies test, and measurements of glucose levels, tri-iodothyronine/thyroxine/thyrotropin, and sex hormone levels. We also checked the couple's chromosomal karyotype and blood type, and we performed an ultrasound scan to confirm that there were no anomalies in the reproductive system. In addition, we carried out routine semen analysis to confirm that there were no potential confounding factors from the patients' partners. Finally, we excluded any patients who had genetic defects or hereditary diseases in their family history. The controls were individuals that had normal ovary and uterus morphology, regular menstrual cycles, and normal reproductive functioning without a history of subfertility treatment. The present study was approved by the Ethics Committee of the Research Institute for Family Planning (no. 2011-10), and informed consent was obtained from all of the participants.

Genotyping

Genomic DNA was extracted from whole-blood samples using the Qiagen Blood Kit (Qiagen), according to the manufacturer's instructions. After extraction, genomic DNA was diluted to a final concentration of 15–20 ng/μl for the genotyping assays. Fifty-five SNPs in the hairpins of the pre-miRNA coding region were selected, and they included 16 sites in the mature miRNA coding region, 18 SNPs in the miRNA complementary sequence of mature miRNA, 12 SNPs in the loop, and nine SNPs in the basal stem (Table 1). The SNPs in the pre-miRNA coding region were analyzed by allele-specific MALDI-TOF mass spectrometry assay using the Sequenom (San Diego, CA, USA) MassARRAY iPLEX platform (Jurinke *et al.* 2002). Primers for the amplification and extension reactions were designed using the MassARRAY Assay Design version 3.1 Software (Sequenom). SNP genotypes were obtained according to the iPLEX protocol provided by the manufacturer. Genotyping quality was examined by a detailed QC procedure that consisted of a >95% successful call rate, the duplicate calling of genotypes, internal positive control samples, and Hardy–Weinberg equilibrium (HWE) testing.

Secondary structure prediction

The secondary structure of the pre-miRNA sequence was predicted using the RNAfold webserver (http://rna.tbi.univie.ac.at/cgi-bin/RNAfold.cgi).

Plasmid construction and transfection

To construct pre-*MIR423* and its SNPs vectors, fragments that corresponded to pre-*MIR423* and its flanking regions were amplified from human genomic DNA and cloned into the pCR3.1 vector (Invitrogen). The sequences of the vectors were confirmed by direct sequencing, and the only difference was in the SNP sites. The pCR3.1-based plasmid, *MIR423* mimic, and *MIR423* inhibitor were transfected into cells by using lipofectamine 2000 (Invitrogen) according to the manufacturer's instructions. To generate 3′-UTR luciferase reporter, a partial sequence of the 3′-UTR from *PA2G4* was cloned into the pGLO vector (Promega; designated as wt-*PA2G4*). Mutant *MIR423* target sites in the 3′-UTR of *PA2G4* were used as corresponding controls (designated as mut-*PA2G4*). The *Pa2g4* 3′-UTR and *PA2G4* 3′-UTR mutant sequences were amplified by PCR from human genomic DNA using the following primers: wt-*PA2G4-SacI* forward: GAGAGCTC-CAACCACGGAAGACTACTTTA, wt-*PA2G4-XbaI* reverse: GACTCTAGATAAATGAAGGCTCCAGCTCC; mut-*PA2G4*-SacI forward: ATTCAGGCTGTCCAGTCAGGTATCTCCGATTTT, mut-*PA2G4*-XbaI reverse: ATACCTGACTGGACAGCCTGAAT-CAGATGAGGA. After being double-digested with *SacI* and *XbaI*, the PCR products were cloned into the downstream of the stop codon of the luciferases gene in the pGLO vector, and the constructs were verified by sequencing.

Quantitative RT-PCR

Total RNA was extracted using Trizol reagent (Invitrogen). The expression of *MIR423* was detected by TaqMan miRNA Real-Time RT-PCR. Total RNA was reverse-transcribed by the TaqMan MicroRNA Reverse Transcription Kit (Applied Biosystems). The acquired single-strand cDNA were amplified by the TaqMan Universal PCR Master Mix (Applied Biosystems) and by the miRNA-specific TaqMan MGB probes for *MIR423* and *U6* (Applied Biosystems). The *U6* was used as an internal control. The expression of *PA2G4* was detected by real-time RT-PCR. Total RNA was reverse-transcribed by the iScript cDNA Synthesis Kit (Bio-Rad). The single-strand cDNA were amplified by a FastStart Universal SYBR Green Master (Roche) and the following primers: forward: 5′-GTTGCCCACTCATTTAACTGC-3′; reverse: 5′-GAGCTGAC-GAGAACATCCAC-3′. Glyceraldehyde-3-phosphate dehydrogenase (*Gapdh*) was used as an endogenous control. Each sample in each group was tested in triplicate, and the experiment was repeated three times.

Cell proliferation assays

Cell proliferation was estimated by BrdU assay. HEC-1b cells were seeded in 24-well plates at low density (5×10^3) in DMEM culture and were allowed to attach overnight. The cells were then transfected with pre-*MIR423* and its SNP vectors. There were three wells in each treatment group. After 48 h of transfection, the cells were incubated with rat monoclonal anti-BrdU (1:400; Abcam, Cambridge, UK) and then with Alexa Fluor 594 donkey anti-rat IgG (1:200; Invitrogen). Cells were viewed under an Eclipse TE2000-U fluorescence microscope (Nikon). To evaluate the specificity of the

Table 1 Polymorphism site selection.

MIR name	SNP	Allele	Location	Reference mature MIR
MIR71	rs76662330	G/T	Mature miR	*MIR71**
MIR92B	rs12759620	C/G	Mature miR	*MIR92B*
MIR568	rs28632138	G/T	Mature miR	*MIR568*
MIR1255B1	rs6841938	A/G	Mature miR	*MIR1255B*
MIR585	rs62376935	C/T	Mature miR	*MIR585*
MIR449B	rs10061133	A/G	Mature miR	*MIR449B*
MIR608	rs4919510	C/G	Mature miR	*MIR608*
MIR938	rs12416605	C/T	Mature miR	*MIR938*
MIR412	rs61992671	A/G	Mature miR	*MIR412*
MIR1268	rs28599926	C/T	Mature miR	*MIR1268*
MIR627	rs2620381	A/C	Mature miR	*MIR627*
MIR940	rs35356504	−/C	Mature miR	*MIR940*
MIR548H3	rs9913045	A/G	Mature miR	*MIR548H*
MIR122	rs41292412	C/T	Mature miR	*MIR122*
MIR520C	rs7255628	C/G	Mature miR	*MIR520C5P*
MIR499	rs3746444	A/G	Mature miR	*MIR4993P*
MIR564	rs2292181	C/G	miR complementary	*MIR564*
MIR146A	rs2910164	C/G	miR complementary	*MIR146A*
MIR548A1	rs12197631	G/T	miR complementary	*MIR5483P*
MIR1206	rs2114358	A/G	miR complementary	*MIR1206*
MIR603	rs11014002	C/T	miR complementary	*MIR603*
MIR604	rs2368393	A/G	miR complementary	*MIR604*
MIR604	rs2368392	A/G	miR complementary	*MIR604*
MIR619	rs34651680	−/G	miR complementary	*MIR619*
MIR1178	rs7311975	C/T	miR complementary	*MIR1178*
MIR618	rs2682818	A/C	miR complementary	*MIR618*
MIR453	rs56103835	C/T	miR complementary	*MIR453*
MIR625	rs12894182	A/C	miR complementary	*MIR625*
MIR1826	rs62030476	A/G	miR complementary	*MIR1826*
MIR1972	rs57629257	C/T	miR complementary	*MIR1972*
MIR633	rs17759989	A/G	miR complementary	*MIR633*
MIR663	rs28670321	C/T	miR complementary	*MIR663*
MIR28	rs78547906	C/T	miR complementary	*MIR28*
MIR92A1	rs72631821	C/T	miR complementary	*MIR92A*
MIR146A	rs61270459	C/T	Loop	*MIR146A*
MIR1274A	rs318039	C/T	Loop	*MIR1274A*
MIR581	rs788517	A/G	Loop	*MIR581*
MIR96	rs41274239	A/G	Loop	*MIR96*
MIR1307	rs7911488	A/G	Loop	*MIR1307*
MIR1265	rs11259096	C/T	Loop	*MIR1265*
MIR656	rs58834075	C/T	Loop	*MIR656*
MIR27A	rs895819	C/T	Loop	*MIR27A*
MIR639	rs45556632	C/G	Loop	*MIR639*
MIR516B2	rs10670323	−/AAAGA	Loop	*MIR516B*
MIR5211	rs2561251	A/G	Loop	*MIR521*
MIR650	rs11558654	A/T	Loop	*MIR650*
MIR18A	rs41275866	C/G	Basal stem	*MIR18A*
MIR423	rs6505162	A/C	Basal stem	*MIR423*
MIR646	rs6513496	C/T	Basal stem	*MIR646*
MIR11	rs6122014	C/T	Basal stem	*MIR1*
MIR605	rs2043556	A/G	Basal stem	*MIR605*
MIR1289	rs35296450	C/G	Basal stem	*MIR1289*
MIR577	rs34115976	C/G	Basal stem	*MIR577*
MIR492	rs2289030	C/G	Basal stem	*MIR492*
MIR12831	rs57111412	A/G	Basal stem	*MIR1283*

* Represents the passenger strand.

antibodies, negative control staining was performed by substituting normal rat serum for the primary antibody.

Flow cytometry analysis

Cell apoptosis was detected by flow cytometry analysis. We harvested the cells after 48 h of transfection. Annexin V-FITC, binding buffer, and PI were proportionally mixed. Fifty microliters of mixture was added to each sample, which was then incubated for 15 min at room temperature. The samples were analyzed at a rate of 8000 events per second by flow cytometry (BD Biosciences, San Diego, CA, USA). Each treatment was repeated twice, and the experiment was repeated three times.

Cell migration and invasion assays

HEC-1b cells were transfected with pCR3.1, pCR3.1-MIR423-C/C, pCR3.1-MIR423-A/A, or pCR3.1-MIR423-C/A. Cells were

harvested after 48 h of transfection. The transfected cells (1×10^5), which were contained in 0.5 ml media without serum or growth factors, were added to the top of 8 μm porous chamber inserts (Corning, Corning, NY, USA) and placed in wells filled with 0.75 ml of medium supplemented with 10% FCS for the migration assays. Matrigel (BD Biosciences) was added to the top of 8 μm porous membrane chambers (Corning) and incubated at room temperature until the matrigel solidified; then, cells (1×10^5) were seeded on top of the matrigel-coated membrane for the invasion assays. After 20 h of incubation, the cells that remained on the insert top layers were removed with a cotton swab as recommended by the manufacturer. Cells in the bottom of the 8 μm porous chamber inserts were fixed by 4% paraformaldehyde solution (Sigma–Aldrich) and stained with hematoxylin and eosin (Sigma–Aldrich). The membranes were photographed under a light microscope, and the cells that passed through the membrane were counted from five different fields per sample, which were selected in a random manner, at 200× magnification.

Dual-luciferase assay

293T cells were seeded in 48-well plates overnight and then transfected by lipofectamine 2000 (Invitrogen). Two days later, the cells were harvested and assayed with the dual-luciferase assay (Promega). Each treatment was performed in triplicate, and there were three independent experiments. The results are expressed as relative luciferase activity (firefly luc/renilla luc).

Statistical analysis

The HWE was determined using a standard χ^2 test (df = 1) to compare the observed frequency with the expected frequency in controls. Allele and genotype frequencies and ORs were calculated online using the SHEsis Software platform (http://analysis.bio-x.cn) (Shi & He 2005, Li *et al*. 2009). The data from the qRT-PCR, cell proliferation, migration, invasion, and dual-luciferase assays were analyzed by one-way ANOVA followed by an least significant difference *post hoc* test and Tukey's test using SPSS Software version 16.0 (SPSS, Inc.). The values are shown as means ± S.E.M. The differences were considered statistically significant at $P<0.05$.

Results

Genetic case–control association study

To explore the relationship between miRNA SNPs and URPL, the genotyping of 55 SNPs in the pre-miRNA coding region were analyzed by allele-specific MALDI-TOF mass spectrometry assay using the Sequenom MassARRAY iPLEX platform. The genotyping success rate was 96.7%. The genotype frequencies of rs6505162 of *MIR423*, rs62030476 of *MIR1826*, and rs9913045 of *MIR548H3* were not significantly different among the controls, as measured by HWE ($P=0.45$, 0.92, 0.97 respectively). The allele frequencies and associated ORs (95% CIs) for the RPL cases and controls are presented in Table 2. Significant differences were found in the allele distributions of these three SNPs ($P<0.01$, $P<0.01$, and $P=0.041$ respectively). Overall, the variant A allele of rs6505162 (OR 1.68, 95% CI 1.14–2.46), the G allele of rs62030476 (OR 6.72, 95% CI 2.49–18.09), and the A allele of rs9913045 (OR 1.42, 95% CI 1.01–2.00) were associated with an increased risk of RPL as compared to the control group.

MIR423 *secondary structure prediction*

Recent studies have shown that *MIR1826* is not an miRNA (http://www.mirbase.org/cgi-bin/mirna_summary.pl?org=hsa), so we did not predict the secondary structure of *MIR1826*. The secondary structures of about 500 bp pre-*MIR423* and pre-*MIR548H3* sequences, including pre-miRNAs and 200 bp upstream and downstream, were predicted using the RNAfold webserver (http://rna.tbi.univie.ac.at/cgi-bin/RNAfold.cgi). The rare allele A in pre-*MIR423* caused an apparent change in loop size and structure as well as a decrease in the predicted ΔG from −135.50 to −119.35 kcal/mol (Fig. 1A). However, the predicted secondary structure and ΔG were not significantly different between the G allele and the A allele in pre-*MIR548H3* (Fig. 1B). ΔG here refers to the free energy of the thermodynamic ensemble, which in some sense represents the thermodynamic stability of the secondary structure. Therefore, we speculate that rs6505162 in pre-*MIR423* may impact the function of mature *MIR423*.

MIR423 *rs6505162 affects* MIR423 *expression*

Because the SNP rs6505162 was located in the pre-*MIR423* coding region, we speculated whether the SNP rs6505162 could alter the production of mature *MIR423*. The effects of C/A polymorphism of rs6505162 on the production of mature *MIR423* were analyzed by TaqMan miRNA Real-Time RT-PCR (Fig. 2). The expression levels of mature *MIR423* in the CC homozygote ($P<0.05$),

Table 2 Case–control analysis of SNP sites in the MIR coding region.

SNP		Frequency		OR (95% CI)	HWE	*P*
rs6505162 (*MIR423*)	Case	A (23.5%)	C (77.9%)	A 1.68 (1.14, 2.46)	0.68	<0.01
	Control	A (15.5%)	C (84.5%)	C 0.60 (0.41, 0.87)	0.45	
rs62030476 (*MIR1826*)	Case	A (81.6%)	G (18.4%)	G 6.72 (2.49, 18.09)	0.84	<0.01
	Control	A (97.0%)	G (3.0%)	A 0.61 (0.38, 0.98)	0.92	
rs9913045	Case	A (34.5%)	G (65.5%)	A 1.42 (1.01, 2.00)	0.37	0.041
(*MIR548H3*)	Control	A (27.0%)	G (73.0%)	G 0.70 (0.50, 0.99)	0.97	

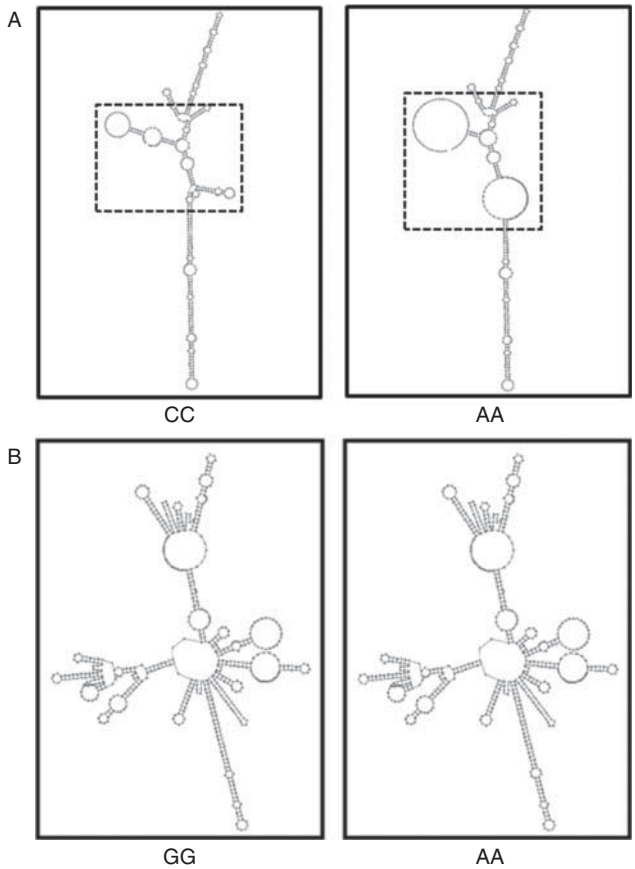

Figure 1 Secondary structure prediction of miRNAs. The RNAfold webserver (http://rna.tbi.univie.ac.at/cgi-bin/RNAfold.cgi) was used to predict the secondary structures of pre-*MIR423* (A) and pre-*MIR548H3* (B).

AA homozygote ($P<0.01$), and C/A heterozygosity ($P<0.01$) were significantly higher than that in the pCR3.1 empty vector, which implies that the constructs of WT and mutant *MIR423* could effectively produce mature *MIR423*. The AA homozygote obviously enhanced the expression level of mature *MIR423* as compared to the CC homozygote ($P<0.01$). Although the mature *MIR423* level is lower in C/A heterozygosity of rs6505162 than it is in the AA homozygote, it was significantly increased by C/A heterozygosity of rs6505162 as compared to the CC homozygote ($P<0.01$). These results suggest that C to A substitution in rs6505162 of *MIR423* promotes the production of mature *MIR423*.

C to A substitution in the rs6505162 polymorphism inhibits cell proliferation

HEC-1b cells were transfected with pCR3.1, pCR3.1-MIR423-C/C, pCR3.1-MIR423-A/A, or pCR3.1-MIR423-C/A. After 48 h, cell proliferation was determined by BrdU assay (Fig. 3). The proliferation ability in the AA homozygote was significantly lower than that in the CC homozygote ($P<0.01$) and the empty pCR3.1 vector ($P<0.01$). C/A heterozygosity of rs6505162 may better facilitate cell viability as compared to the AA homozygote ($P<0.01$), whereas the cell proliferation ability in the C/A heterozygosity of rs6505162 was equal to that in the CC homozygote and the empty pCR3.1 vector. These results suggest an association of A allele with the inhibition of cell viability.

MIR423 *rs6505162 impacts cell apoptosis*

To further explore the role of rs6505162 of *MIR423* in controlling cell growth, cell apoptosis was determined by flow cytometry analysis (Fig. 4). The percentages of early apoptotic cells (annexin V-FITC-positive) transfected with pCR3.1, pCR3.1-MIR423-C/C, pCR3.1-MIR423-A/A, or pCR3.1-MIR423-C/A were about 6.0, 4.0, 2.5, and 1.9%, respectively. The percentages of late apoptotic cells (annexin VFITC/PI-positive) transfected with pCR3.1, pCR3.1-MIR423-C/C, pCR3.1-MIR423-A/A, and pCR3.1-MIR423-C/A were about 1.9, 1.4, 1.2, and 0.8% respectively. These results show that rs6505162 of *MIR423* has no significant effect on cell apoptosis.

MIR423 *rs6505162 impacts cell migration and invasion*

To further research the effect of *MIR423* rs6505162 on cell behavior, we analyzed the influence of *MIR423* rs6505162 on cell migration and invasion (Figs 5 and 6). The CC homozygote had no significant effect on cell

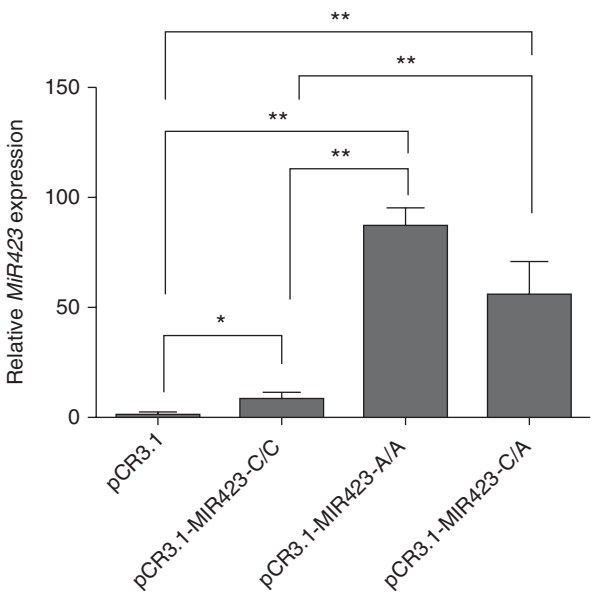

Figure 2 *MiR423* expression from different genotypes in transfected cells. The *MIR423* level was detected in cells that were transfected with pCR3.1-MIR423-C/C, pCR3.1-MIR423-A/A, or pCR3.1-MIR423-C/A by TaqMan miRNA Real-Time RT-PCR. *U6* snRNA was used as an internal control. The relative level of *MIR423* was normalized to *U6*. *$P<0.05$ and **$P<0.01$.

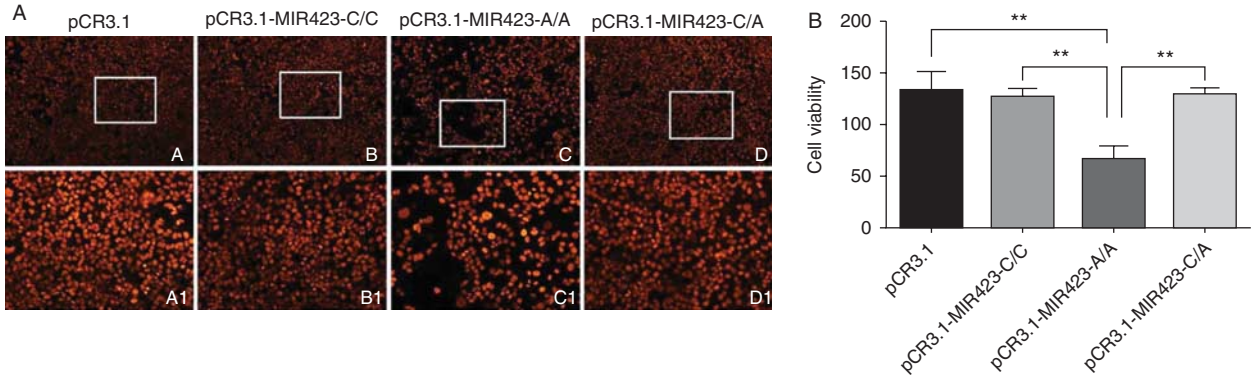

Figure 3 Cell proliferation as detected by BrdU assay. PCR3.1, pCR3.1-MIR423-C/C, pCR3.1-MIR423-A/A, or pCR3.1-MIR423-C/A was transfected into HEC-1b cells. After 48 h of transfection, cell proliferation was determined by BrdU assay. All of the experiments were performed at least three times. $^{**}P<0.01$.

migratory capacity in HEC-1b cells. The AA homozygote reduced cell migratory capacity as compared to the CC homozygote, but this finding was not statistically significant. However, cell migratory capacity was significantly inhibited by the C/A heterozygosity of rs6505162 as compared to the CC homozygote and the empty vector ($P<0.01$; Fig. 5). Additionally, the invasion assay indicated that the invasive capacity was not significantly different among the CC homozygote, the AA homozygote, and the C/A heterozygosity of rs6505162 (Fig. 6). These findings suggest that *MIR423* rs6505162 may suppress cell migration.

MIR423 *affects the expression of* PA2G4 *in HEC-1b* in vitro

To analyze the possible molecular mechanisms in which *MIR423* is involved, its target genes were studied. An online search of *MIR423* targets in the TargetScan (www.targetscan.org), miRDB (http://mirdb.org/miRDB/index.html), and miRanda (http://www.microrna.org) databases showed that there was a conservative 7nt *MIR423* responsive element in the 3′-UTR of *PA2G4* (Fig. 7A). A key role of miRNA is to regulate the expression of target genes, so we analyzed the expression pattern of *PA2G4* when *MIR423* levels were altered.

HEC-1b cells were transfected with *MIR423* mimic or inhibitor to analyze the effects of *MIR423* expression on endogenous *PA2G4* expression. PA2G4 protein levels detected by western blot were significantly down-regulated by *MIR423* mimic as compared to pre-MIR control ($P<0.05$), they were and up-regulated by *MIR423* inhibitor as compared to anti-MIR control ($P<0.05$; Fig. 8A). Furthermore, qRT-PCR was used to detect *PA2G4* mRNA levels. *MIR423* mimic significantly decreased *PA2G4* mRNA levels ($P<0.01$), whereas *MIR423* inhibitor markedly increased *PA2G4* mRNA levels ($P<0.01$; Fig. 8B). These findings show that the mRNA and protein levels of endogenous *PA2G4* can be regulated by *MIR423*.

MIR423 *directly targets the 3′-UTR of* PA2G4

To validate *PA2G4* as the direct target of *MIR423*, we established a luciferase reporter assay system. The 3′-UTR of *PA2G4*, which contains *MIR423* target sites,

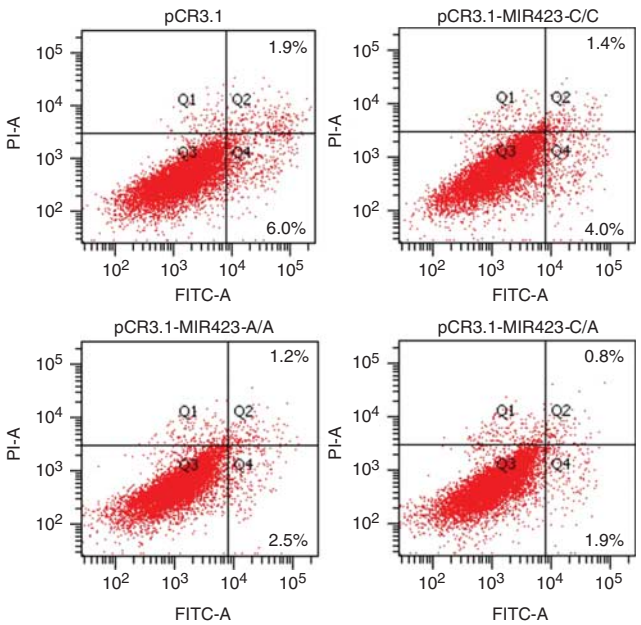

Figure 4 Cell apoptosis as detected by flow cytometry analysis. PCR3.1, pCR3.1-MIR423-C/C, pCR3.1-MIR423-A/A, or pCR3.1-MIR423-C/A was transfected into HEC-1b cells. After 48 h of transfection, single-cell suspension was prepared and stained with annexin V/PI and subjected to flow cytometry analysis. Lower left quadrant: viable cells (annexin V-FITC and PI negative). Lower right quadrant: early apoptotic cells (annexin V-FITC positive and PI negative). Upper right quadrant: late apoptosis/necrosis cells (annexin V-FITC and PI positive). The percentages of early and late apoptotic cells (representatives of three separate experiments) are shown in the lower right and upper right panels respectively.

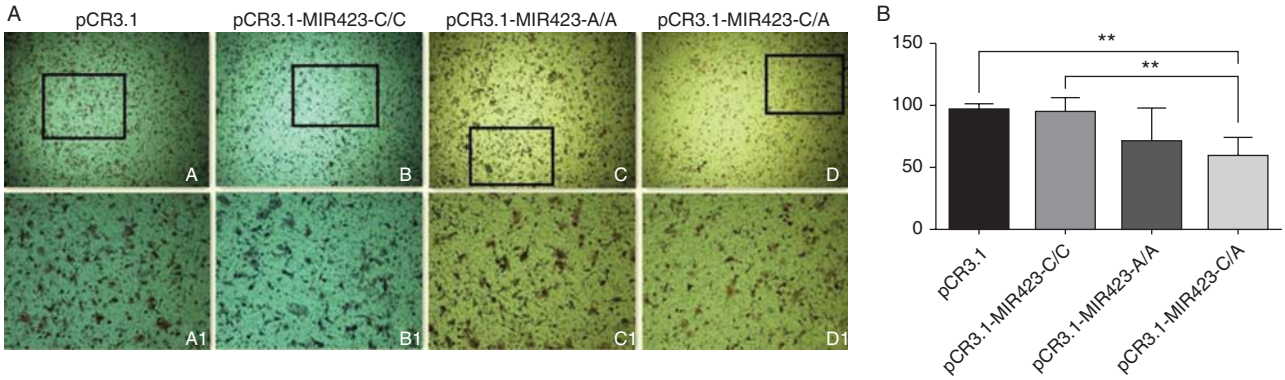

Figure 5 Cell migration in HEC-1b cells. Cell migratory capacity was detected in HEC-1b cells transfected with pCR3.1, pCR3.1-MIR423-C/C, pCR3.1-MIR423-A/A, or pCR3.1-MIR423-C/A (A). Cells that had migrated to the bottom of the Transwell filter were quantified by counting the number of cells that passed through the membrane from five different fields per sample, which were selected in a random manner, at 200× magnification (B). Data are expressed as the means (± S.E.M.) of three independent experiments. $^{**}P<0.01$.

was PCR-amplified from human genomic DNA and cloned into pmirGLO. *MIR423* mimic and inhibitor were co-transfected with wt-*PA2G4* (Fig. 7B). Compared to the pre-MIR control, the luciferase activity was significantly decreased by the *MIR423* mimic ($P<0.01$). When cells were transfected with the *MIR423* inhibitor, the luciferase activity had an obvious upward trend as compared to the anti-MIR control.

In order to confirm the binding sites for *MIR423* in the 3′-UTR of *PA2G4*, we mutated the partial seed sequence in the 3′-UTR of *PA2G4*. As shown in Fig. 7C, co-transfections of *MIR423* mimics and wt-*PA2G4* significantly reduced the enzyme activity as compared to co-transfections of *MIR423* mimics and mut-*PA2G4* ($P<0.01$), which suggests that the mutation of the seed sequence could disrupt the binding of *MIR423* to the 3′-UTR of *PA2G4*. All of these data show that *PA2G4* may be the direct target gene of *MIR423*.

The expression pattern of PA2G4 *in the decidual tissues in patients with two or more consecutive missed abortions*

The expression levels of *PA2G4* in the decidual tissues in patients with two or more consecutive missed abortions were detected by qRT-PCR and western blot (Fig. 9). The mRNA level of *PA2G4* was significantly decreased in the RPL group as compared to the control group ($P<0.05$). The protein levels of PA2G4 were lower in the RPL group than they were in the control group, but this finding was not statistically significant.

MIR423 *rs6505162 influences the expression of the* MIR423 *target gene*

In the experiments described earlier in the present study, *PA2G4* was confirmed to be the direct target gene of *MIR423*. The results from the TaqMan miRNA Real-Time

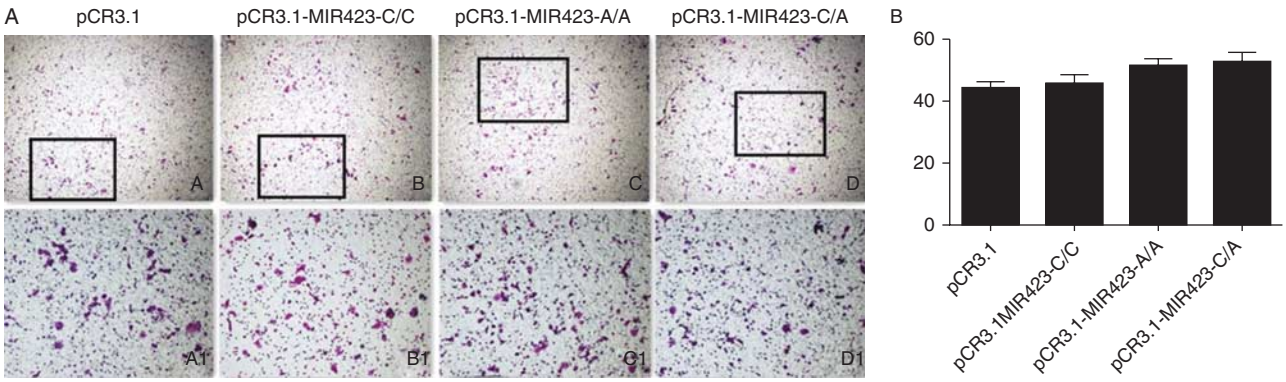

Figure 6 Cell invasion in HEC-1b cells. Cell invasive capacity was detected in HEC-1b cells transfected with pCR3.1, pCR3.1-MIR423-C/C, pCR3.1-MIR423-A/A, or pCR3.1-MIR423-C/A (A). Cells that had migrated to the bottom of the Transwell filter were quantified by counting the number of cells that passed through the membrane from five different fields per sample, which were selected in a random manner, at 200× magnification (B). Data are expressed as the means (± S.E.M.) of three independent experiments.

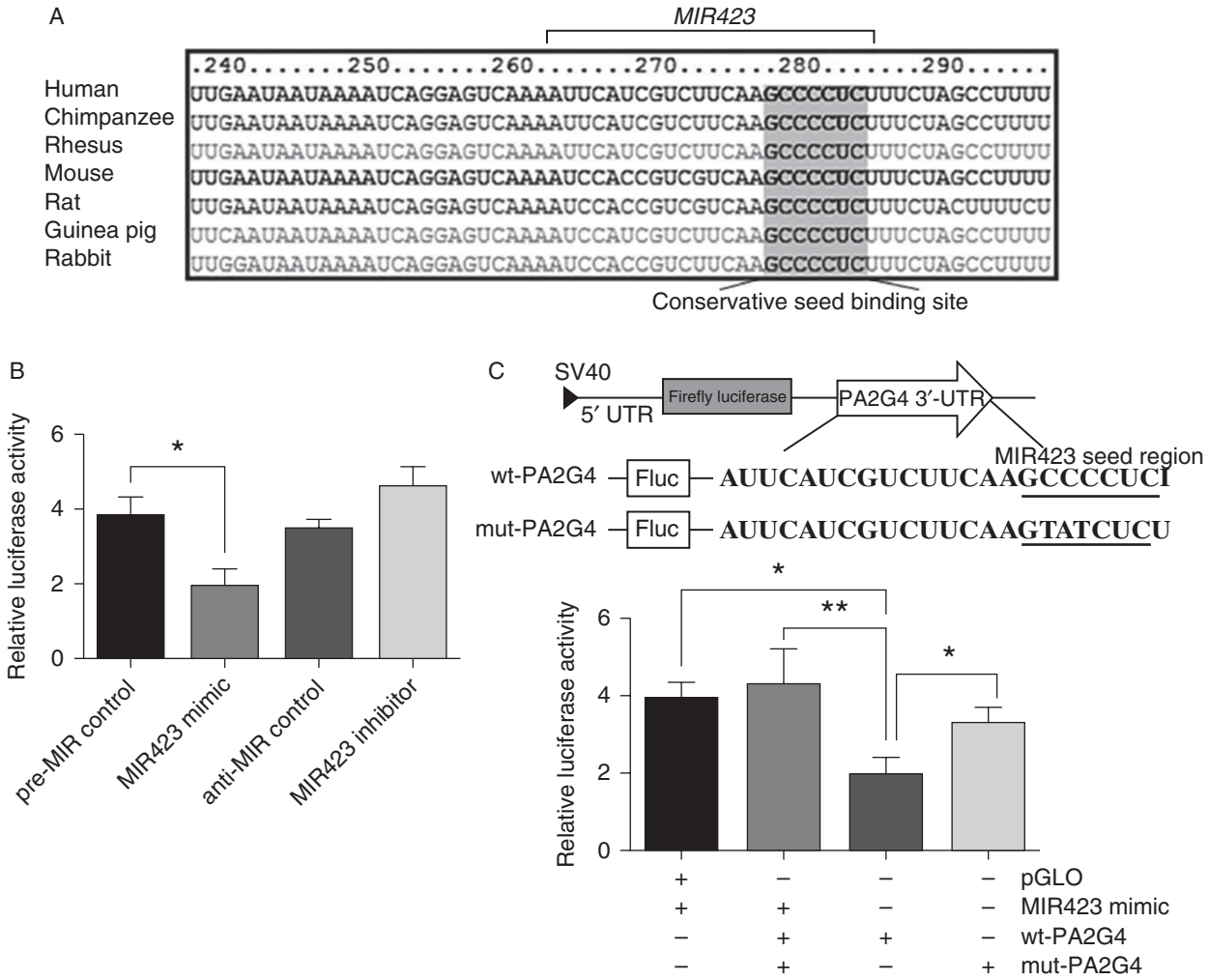

Figure 7 The prediction and confirmation of the *MIR423* target gene. *MIR423* binding sites in the 3′-UTR of *PA2G4* were compared in cross-species (A). HEC-1b cells were co-transfected with a *MIR423* mimic, a *MIR423* inhibitor, a pre-MIR control, an anti-MIR control, and wt-*PA2G4* for dual-luciferase assay (B). HEC-1b cells were co-transfected with *MIR423* and wt- or mut-*PA2G4* for dual-luciferase assay (C). Mut-*PA2G4* (mutating putative *MIR423* binding region in the 3′-UTR of *PA2G4*) was used as a control. pRL-TK containing Renilla luciferase was co-transfected for data normalization. *$P<0.05$ and **$P<0.01$.

RT-PCR showed that rs6505162 of *MIR423* increases the expression of mature *MIR423*. In order to address the question of whether *MIR423* rs6505162 can affect *PA2G4* expression, the different genotypes of *MIR423* rs6505162 were co-transfected with either wt-*PA2G4* or mut-*PA2G4* (Fig. 10). Mut-*PA2G4* was used as a negative control. Compared to the negative control, luciferase activity was significantly decreased in cells that were co-transfected with pCR3.1-MIR423-C/C, pCR3.1-MIR423-A/A, pCR3.1-MIR423-C/A, and wt-*PA2G4* ($P<0.01$), which implies that the seed sequence in 3′-UTR of *PA2G4* is specific to *MIR423*. When cells were co-transfected with wt-*PA2G4* and the different genotypes of *MIR423* rs6505162, the AA homozygote more significantly suppressed the luciferase activity than the CC homozygote did ($P<0.01$), and the C/A heterozygosity of rs6505162 slightly diminished luciferase activity as compared to the CC homozygote and increased luciferase activity as compared to AA homozygote. These results show that the A allele can effectively repress the expression of *PA2G4* by up-regulating *MIR423* levels.

Discussion

To our knowledge, the present study is the first to provide a general view of the relationship between potentially functional polymorphisms in pre-miRNAs and RPL susceptibility, although many SNPs in miRNAs sequences have been identified as having a strong relationship to disease (Saunders *et al.* 2007, Hu *et al.* 2008, Jazdzewski *et al.* 2008, 2009).

The polymorphisms in miRNA precursors and the mature miRNA coding region may have more significant

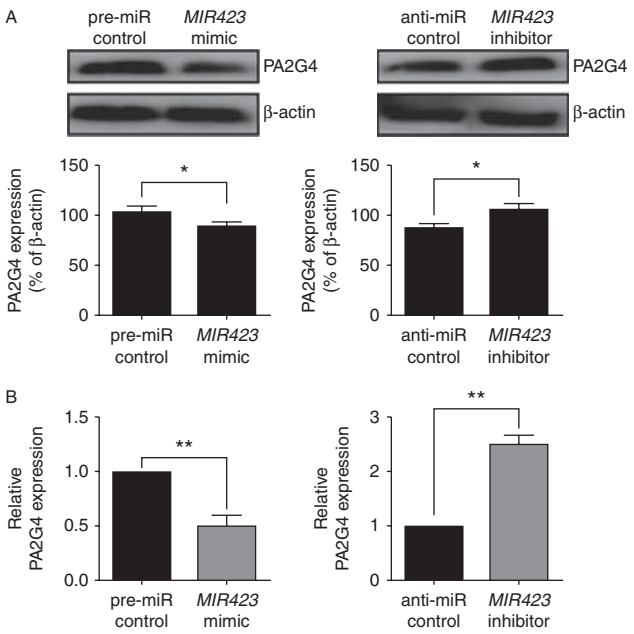

Figure 8 *MIR423* regulates *PA2G4* expression. (A) PA2G4 protein levels in *MIR423* mimic- or *MIR423* inhibitor-treated HEC-1b cells was detected by western blot. The bands were analyzed using the Quantity One analyzing system (Bio-Rad). β-actin served as an internal control. The black histogram represents the optical densities of the signals quantified by densitometric analysis. (B) The expression of *PA2G4* mRNA in *MIR423* mimic- and *MIR423* inhibitor-treated HEC-1b cells was detected by qRT-PCR. β-actin served as an internal reference. $^{*}P<0.05$ and $^{**}P<0.01$.

effects on miRNA expression and function than do those in the primary miRNA coding region (Kontorovich *et al.* 2010). Therefore, in the present study, we chose 55 SNPs in the hairpins of the pre-miRNA coding region in order to study the relationship between the polymorphisms of miRNAs and RPL susceptibility. The 55 SNPs are located in 54 miRNA coding regions. The reasons why we chose these miRNA SNPs were as follows: first, our previous experiments found that many of the miRNA SNPs listed in the NCBI's Short Genetic Variations database (dsSNP) do not exist in the Chinese population, so we chose miRNA SNPs that do exist in the Chinese population. For example, an SNP in *MIR146A* has been found to be associated with improved lung function and milder disease stages in Han Chinese people (Wang *et al.* 2015). Likewise, rs4919510 in pre-*MIR608* has been associated with increased recurrence-free survival in patients with colorectal cancer in Chinese people (Xing *et al.* 2012). Second, implantation failure is one of major reasons for RPL. We therefore chose some miRNAs that have been shown to be differentially expressed in implantation vs pre-implantation rat uteri, such as *MIR92A*, *MIR92B*, *MIR1268*, and so on. (Xia *et al.* 2014*a*,*b*). In addition, there are striking similarities in cell behavior between invasive trophoblastic cells during embryo implantation and invasive cancer cells (Murray & Lessey 1999). We consequently chose some miRNAs that have been shown to execute functions in tumorigenesis, such as *MIR568*, *MIR1255B*, *MIR585*, and so on (Hidaka *et al.* 2012, Xiao *et al.* 2012, Leidner *et al.* 2013).

The 55 miRNA SNPs were detected by allele-specific MALDI-TOF mass spectrometry assay. Significant differences were found in the allele distributions of *MIR423* rs6505162, *MIR1826* rs62030476, and *MIR548H3* rs9913045 between RPL cases and controls. The prediction of a secondary structure showed that loop size, structure, and predicted ΔG were altered by the rare allele A in the pre-*MIR423* coding region. However, the predicted secondary structure and ΔG were not significantly different between the G allele and the A allele in pre-*MIR548H3*. In addition, recent studies have shown that *MIR1826* is not an miRNA (http://www.mirbase.org/cgi-bin/mirna_summary.pl?org=hsa). Therefore, we chose to study rs6505162 in pre-*MIR423*.

The SNP rs6505162 is located in pre-*MIR423*, so we analyzed the impact of C/A polymorphism of rs6505162

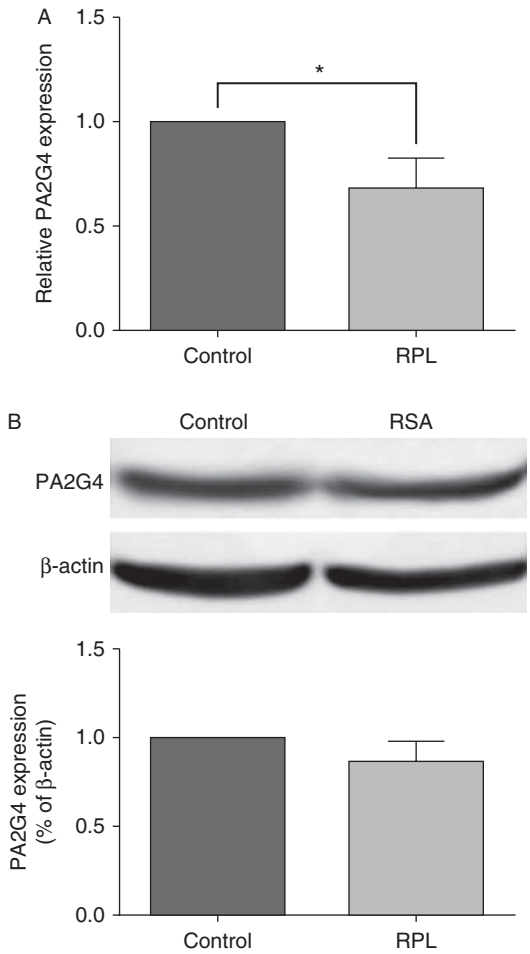

Figure 9 The expression of *PA2G4* in the decidual tissues of patients with two or more consecutive missed abortions. The expression level of *PA2G4* in the decidual tissues was detected by qRT-PCR (A) and western blot (B). β-actin served as an internal reference. $^{*}P<0.05$.

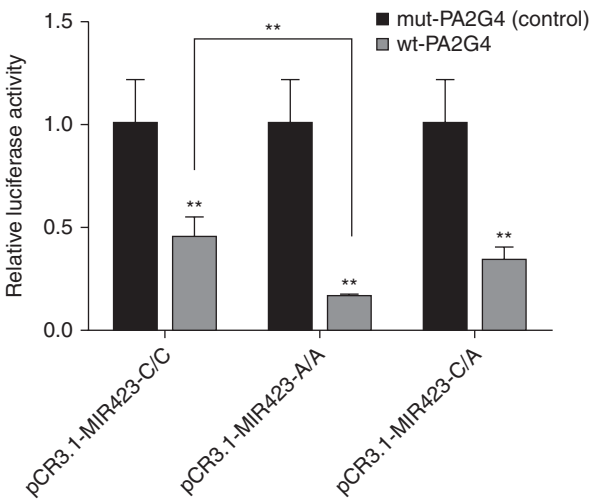

Figure 10 The impact of SNP on *MIR423* target genes as detected by dual-luciferase assay. The relative luciferase activity of reporter vector with 3′-UTR of *PA2G4* containing normal or mutated target sites was detected in the presence of pCR3.1-MIR423-C/C, pCR3.1-MIR423-A/A, or pCR3.1-MIR423-C/A. Mut-*PA2G4* (mutating putative *MIR423* binding region in the 3′-UTR of *PA2G4*) was used as a control. $^{**}P<0.01$.

on the production of mature *MIR423*. The expression level of *MIR423* in the AA homozygote was markedly higher than that in the CC homozygote. Although the mature *MIR423* level was lower in the C/A heterozygosity of rs6505162 than in the A allele, it was significantly increased by the C/A heterozygosity of rs6505162 as compared to the CC homozygote. These results suggest that the rare allele A in pre-*MIR423* contributes to the production of mature *MIR423*, which is similar to the polymorphisms of *MIR125A* and has been shown to be associated with an increased risk of RPL in the Han Chinese population (Hu *et al.* 2011). The rs6505162 C >A in *MIR423* has been identified as a biomarker for many diseases. For example, Smith *et al.* (2012) showed than the C >A polymorphism located in the pre-miRNA region of *MIR423* is associated with reduced breast cancer. Rs6505162 in pre-*MIR423* was also identified as being significantly associated with recurrence-free survival and overall survival in patients with colorectal cancer (Xing *et al.* 2012). Hsa-*MIR423* rs6505162 C >A might also be associated with a significantly increased risk of esophageal squamous cell carcinoma in patients who smoke (Yin *et al.* 2013). Additionally, *MIR423* C>A has been associated with an increased risk of primary ovarian insufficiency (Rah *et al.* 2015). These previous studies imply that *MIR423* rs6505162 has the potential to become a biomarker for the diagnosis of many clinical diseases.

In the present study, the effects of *MIR423* rs6505162 on cell behavior were investigated in order to better understand the functional significance of the polymorphism of rs6505162 in the *MIR423* coding region. BrdU assay indicated that mutant *MIR423* (an AA homozygote) exhibited significantly lower proliferation ability than that of WT *MIR423* (a CC homozygote). The apoptosis levels of HEC-1b were not significantly different among the CC homozygote, AA homozygote, and C/A heterozygosity of rs6505162. The cell migratory capacity was reduced by mutant *MIR423* as compared to WT *MIR423*. However, rs6505162 of *MIR423* did not have a significant effect on cell invasive capacity. All of these results show that C to A substitution in *MIR423* rs6505162 inhibits cell proliferation and migratory capacity.

To further explore the possible molecular mechanisms by which *MIR423* rs6505162 regulates *MIR423* function, we analyzed the binding status of *MIR423* rs6505162 and its target gene by luciferase reporter assay. An online search of *MIR423* targets in the TargetScan, miRDB, and miRanda databases provided a large number of putative mRNA targets. Among them, we focused on *PA2G4* for the following reasons: i) the TargetScan, miRDB, and miRanda predictions all showed that there was one *MIR423* responsive element in the 3′-UTR of *PA2G4*; ii) because *MIR423* rs6505162 can affect cell proliferation, we chose target genes of *MIR423* near proliferation-related proteins. It has been reported that *PA2G4* is involved in cell proliferation (Radomski & Jost 1995); iii) we found that *PA2G4* expression was down-regulated by the *MIR423* mimic, but the expression level of *PA2G4* was up-regulated by the *MIR423* inhibitor. Thus, *PA2G4* levels were inverted with *MIR423* levels.

A luciferase reporter assay was used to validate whether *MIR423* directly targeted *PA2G4*. In the luciferase assay of transfection with wt-*PA2G4*, luciferase activity was decreased by the *MIR423* mimic and increased by the *MIR423* inhibitor, which suggests that the dysregulation of *MIR423* influenced the binding of *MIR423* and the 3′-UTR of *PA2G4*. Mutating seed sequence experiments confirmed that the binding sites in the 3′-UTR of *PA2G4* were specific for *MIR423*. These results confirmed that *PA2G4* is the direct target gene of *MIR423*. When HEC-1b cells were co-transfected with wt-*PA2G4* and a CC homozygote, an AA homozygote, or a C/A heterozygosity of rs6505162, the luciferase activity was more significantly inhibited by the AA homozygote than it was by the CC homozygote, which suggests that the A allele could more effectively suppress the expression of *PA2G4* than the C allele could.

PA2G4 (also known as EBP1, HG4-1, p38-2G4) has been defined as a novel cell cycle specifically modified and proliferation-associated nuclear protein in mammals (Radomski & Jost 1995). *Pa2g4* knockout in mice decreased the expression of insulin-like growth factor 1 (*Igf1*) and increased the expression of growth factor receptor bound protein 10 (*Grb10*) (Zhang *et al.* 2008). Igf1 has been shown to play a critical role in placental function, which stimulates extravillous trophoblast (EVT) cell migration and invasion and thereby influences placental development and fetal growth. Insufficient

invasion of EVT cells into the endometrium leads to pregnancy-related complications, including pregnancy loss (Kabir-Salmani *et al*. 2002, Mayama *et al*. 2013). *Grb10* encodes a signaling adapter protein, is expressed predominantly from the maternally inherited allele, and acts to restrict fetal and placental growth (Charalambous *et al*. 2010).*Grb10* expression in term placenta is significantly negatively correlated with head circumference (Moore *et al*. 2015). Our previous study showed that *Grb10* expression was decreased in rat uteruses during embryo implantation by *Mir199A* and was not beneficial to endometrial development (Xia *et al*. 2014*a*,*b*). In the present study, we confirmed that *PA2G4* is the direct target gene of *MIR423* and is reversely regulated by *MIR423*. The results from the TaqMan miRNA Real-Time RT-PCR showed that C to A substitution in *MIR423* rs6505162 promoted the expression of mature *MIR423*. Additionally, we found that the expression of *PA2G4* was diminished in the decidual tissues of patients with two or more consecutive missed abortions. According to the published reports, the down-regulation of *PA2G4* may suppress *IGF1* expression and enhance *GRB10* levels. Therefore, we speculate that the down-regulation of *PA2G4* by C to A substitution in *MIR423* rs6505162 may result in an insufficient invasion of EVT cells into the endometrium as well as abnormal placental and endometrial development by down-regulating *IGF1* and up-regulating *GRB10,* and this can then lead to spontaneous abortion.

Conclusion

In conclusion, we established the first association between SNPs in *MIR423* and the risk of URPL in a northern Chinese Han population by identifying one functional SNP site in pre-*MIR423*. These findings may provide insight into our understanding of URPL pathogenesis and may suggest a new biomarker for the diagnosis of URPL.

Declaration of interest

The authors declare that there is no conflict of interest that could be perceived as prejudicing the impartiality of the research reported.

Funding

This work was supported by the National Natural Science Foundation of China (grant number 81370720).

References

Charalambous M, Cowley M, Geoghegan F, Smith FM, Radford EJ, Marlow BP, Graham CF, Hurst LD & Ward A 2010 Maternally-inherited Grb10 reduces placental size and efficiency. *Developmental Biology* **337** 1–8. (doi:10.1016/j.ydbio.2009.10.011)

Craig M, Tata P & Regan L 2002 Psychiatric morbidity among patients with recurrent miscarriage. *Journal of Psychosomatic Obstetrics and Gynaecology* **23** 157–164. (doi:10.3109/01674820209074668)

Hidaka H, Seki N, Yoshino H, Yamasaki T, Yamada Y, Nohata N, Fuse M, Nakagawa M & Enokida H 2012 Tumor suppressive microRNA-1285 regulates novel molecular targets: aberrant expression and functional significance in renal cell carcinoma. *Oncotarget* **3** 44–57.

Hinske LC, Galante PA, Kuo WP & Ohno-Machado L 2010 A potential role for intragenic miRNAs on their hosts' interactome. *BMC Genomics* **11** 533. (doi:10.1186/1471-2164-11-533)

Hu Z, Chen J, Tian T, Zhou X, Gu H, Xu L, Zeng Y, Miao R, Jin G, Ma H *et al.* 2008 Genetic variants of miRNA sequences and non-small cell lung cancer survival. *Journal of Clinical Investigation* **118** 2600–2608. (doi:10.1172/JCI32053)

Hu Y, Liu CM, Qi L, He TZ, Shi-Guo L, Hao CJ, Cui Y, Zhang N, Xia HF & Ma X 2011 Two common SNPs in pri-miR-125a alter the mature miRNA expression and associate with recurrent pregnancy loss in a Han-Chinese population. *RNA Biology* **8** 861–872. (doi:10.4161/rna.8.5.16034)

Jazdzewski K, Murray EL, Franssila K, Jarzab B, Schoenberg DR & de la Chapelle A 2008 Common SNP in pre-miR-146a decreases mature miR expression and predisposes to papillary thyroid carcinoma. *PNAS* **105** 7269–7274. (doi:10.1073/pnas.0802682105)

Jazdzewski K, Liyanarachchi S, Swierniak M, Pachucki J, Ringel MD, Jarzab B & de la Chapelle A 2009 Polymorphic mature microRNAs from passenger strand of pre-miR-146a contribute to thyroid cancer. *PNAS* **106** 1502–1505. (doi:10.1073/pnas.0812591106)

Jurinke C, van den Boom D, Cantor CR & Koster H 2002 Automated genotyping using the DNA MassArray technology. *Methods in Molecular Biology* **187** 179–192.

Kabir-Salmani M, Shiokawa S, Akimoto Y, Hasan-Nejad H, Sakai K, Nagamatsu S, Sakai K, Nakamura Y, Hosseini A & Iwashita M 2002 Characterization of morphological and cytoskeletal changes in trophoblast cells induced by insulin-like growth factor-I. *Journal of Clinical Endocrinology and Metabolism* **87** 5751–5759. (doi:10.1210/jc.2002-020550)

Kloosterman WP, Wienholds E, Ketting RF & Plasterk RH 2004 Substrate requirements for let-7 function in the developing zebrafish embryo. *Nucleic Acids Research* **32** 6284–6291. (doi:10.1093/nar/gkh968)

Kontorovich T, Levy A, Korostishevsky M, Nir U & Friedman E 2010 Single nucleotide polymorphisms in miRNA binding sites and miRNA genes as breast/ovarian cancer risk modifiers in Jewish high-risk women. *International Journal of Cancer* **127** 589–597. (doi:10.1002/ijc.25065)

Leidner RS, Li L & Thompson CL 2013 Dampening enthusiasm for circulating microRNA in breast cancer. *PLoS ONE* **8** e57841. (doi:10.1371/journal.pone.0057841)

Li Z, Zhang Z, He Z, Tang W, Li T, Zeng Z, He L & Shi Y 2009 A partition-ligation-combination-subdivision EM algorithm for haplotype inference with multiallelic markers: update of the SHEsis (http://analysis.bio-x.cn). *Cell Research* **19** 519–523. (doi:10.1038/cr.2009.33)

Lytle JR, Yario TA & Steitz JA 2007 Target mRNAs are repressed as efficiently by microRNA-binding sites in the 5′ UTR as in the 3′ UTR. *PNAS* **104** 9667–96729. (doi:10.1073/pnas.0703820104)

Mayama R, Izawa T, Sakai K, Suciu N & Iwashita M 2013 Improvement of insulin sensitivity promotes extravillous trophoblast cell migration stimulated by insulin-like growth factor-I. *Endocrine Journal* **60** 359–368. (doi:10.1507/endocrj.EJ12-0241)

Moore GE, Ishida M, Demetriou C, Al-Olabi L, Leon LJ, Thomas AC, Abu-Amero S, Frost JM, Stafford JL, Chaoqun Y *et al.* 2015 The role and interaction of imprinted genes in human fetal growth. *Philosophical Transactions of the Royal Society of London. Series B, Biological Sciences* **370** 20140074. (doi:10.1098/rstb.2014.0074)

Murray MJ & Lessey BA 1999 Embryo implantation and tumor metastasis: common pathways of invasion and angiogenesis. *Seminars in Reproductive Endocrinology* **17** 275–290. (doi:10.1055/s-2007-1016235)

Practice Committee of American Society for Reproductive Medicine 2013 Definitions of infertility and recurrent pregnancy loss: a committee opinion. *Fertility and Sterility* **99** 63. (doi:10.1016/j.fertnstert.2012.09.023)

Radomski N & Jost E 1995 Molecular cloning of a murine cDNA encoding a novel protein, p38-2G4, which varies with the cell cycle. *Experimental Cell Research* **220** 434–445. (doi:10.1006/excr.1995.1335)

Rah H, Kim HS, Cha SH, Kim YR, Lee WS, Ko JJ & Kim NK 2015 Association of breast cancer-related microRNA polymorphisms with idiopathic primary ovarian insufficiency. *Menopause* **22** 437–443. (doi:10.1097/GME.0000000000000325)

Rai R & Regan L 2006 Recurrent miscarriage. *Lancet* **368** 601–611. (doi:10.1016/S0140-6736(06)69204-0)

Regan L & Rai R 2000 Epidemiology and the medical causes of miscarriage. *Baillières Best Practice & Research. Clinical Obstetrics & Gynaecology* **14** 839–854.

Saunders MA, Liang H & Li WH 2007 Human polymorphism at microRNAs and microRNA target sites. *PNAS* **104** 3300–3305. (doi:10.1073/pnas.0611347104)

Shi YY & He L 2005 SHEsis, a powerful software platform for analyses of linkage disequilibrium, haplotype construction, and genetic association at polymorphism loci. *Cell Research* **15** 97–98. (doi:10.1038/sj.cr.7290286)

Smith RA, Jedlinski DJ, Gabrovska PN, Weinstein SR, Haupt L & Griffiths LR 2012 A genetic variant located in miR-423 is associated with reduced breast cancer risk. *Cancer Genomics & Proteomics* **9** 115–118.

Wang R, Li M, Zhou S, Zeng D, Xu X, Xu R & Sun G 2015 Effect of a single nucleotide polymorphism in miR-146a on COX-2 protein expression and lung function in smokers with chronic obstructive pulmonary disease. *International Journal of Chronic Obstructive Pulmonary Disease* **10** 463–473.

Xia HF, Cao JL, Jin XH & Ma X 2014*a* MiR199a is implicated in embryo implantation by regulating Grb10 in rat. *Reproduction* **147** 91–99. (doi:10.1530/REP-13-0290)

Xia HF, Jin XH, Cao ZF, Hu Y & Ma X 2014*b* MicroRNA expression and regulation in the uterus during embryo implantation in rat. *FEBS Journal* **281** 1872–1891. (doi:10.1111/febs.12751)

Xiao W, Bao ZX, Zhang CY, Zhang XY, Shi LJ, Zhou ZT & Jiang WW 2012 Upregulation of miR-31* is negatively associated with recurrent/newly formed oral leukoplakia. *PLoS ONE* **7** e38648. (doi:10.1371/journal.pone.0038648)

Xing J, Wan S, Zhou F, Qu F, Li B, Myers RE, Fu X, Palazzo JP, He X, Chen Z *et al.* 2012 Genetic polymorphisms in pre-microRNA genes as prognostic markers of colorectal cancer. *Cancer Epidemiology, Biomarkers & Prevention* **21** 217–227. (doi:10.1158/1055-9965.EPI-11-0624)

Yin J, Wang X, Zheng L, Shi Y, Wang L, Shao A, Tang W, Ding G, Liu C & Liu R 2013 Hsa-miR-34b/c rs4938723 T>C and hsa-miR-423 rs6505162 C>A polymorphisms are associated with the risk of esophageal cancer in a Chinese population. *PLoS ONE* **8** e80570. (doi:10.1371/journal.pone.0080570)

Zhang Y, Lu Y, Zhou H, Lee M, Liu Z, Hassel BA & Hamburger AW 2008 Alterations in cell growth and signaling in ErbB3 binding protein-1 (Ebp1) deficient mice. *BMC Cell Biology* **9** 69. (doi:10.1186/1471-2121-9-69)

Received 7 January 2015
First decision 30 January 2015
Revised manuscript received 9 April 2015
Accepted 25 April 2015